Cellular/Molecular

NAD^+ Activates K_{Na} Channels in Dorsal Root Ganglion Neurons

Thomas J. Tamsett,[1] Kelly E. Picchione,[1] and Arin Bhattacharjee[1,2]

[1]Program in Neuroscience and [2]Department of Pharmacology and Toxicology, The State University of New York at Buffalo, Buffalo, New York 14214

Although sodium-activated potassium channels (K_{Na}) have been suggested to shape various firing patterns in neurons, including action potential repolarization, their requirement for high concentrations of Na^+ to gate conflicts with this view. We characterized K_{Na} channels in adult rat dorsal root ganglion (DRG) neurons. Using immunohistochemistry, we found ubiquitous expression of the Slack K_{Na} channel subunit in small-, medium-, and large-diameter DRG neurons. Basal K_{Na} channel activity could be recorded from cell-attached patches of acutely dissociated neurons bathed in physiological saline, and yet in excised inside-out membrane patches, the Na^+ EC_{50} for K_{Na} channels was typically high, ~50 mM. In some cases, however, K_{Na} channel activity remained considerable after initial patch excision but decreased rapidly over time. Channel activity was restored in patches with high Na^+. The channel rundown after initial excision suggested that modulation of channels might be occurring through a diffusible cytoplasmic factor. Sequence analysis indicated that the Slack channel contains a putative nicotinamide adenine dinucleotide (NAD^+)-binding site; accordingly, we examined the modulation of native K_{Na} and Slack channels by NAD^+. In inside-out-excised neuronal patch recordings, we found a decrease in the Na^+ EC_{50} for K_{Na} channels from ~50 to ~20 mM when NAD^+ was included in the perfusate. NAD^+ also potentiated recombinant Slack channel activity. NAD^+ modulation may allow K_{Na} channels to operate under physiologically relevant levels of intracellular Na^+ and hence provides an explanation as to how K_{Na} channel can control normal neuronal excitability.

Introduction

Numerous investigations on sodium-activated potassium channels (K_{Na}) have put forward putative physiological roles for these channels including action potential repolarization, slow afterhyperpolarization, burst firing, and adaptation after repetitive firing (Bhattacharjee and Kaczmarek, 2005). In some neurons, these channels have been suggested to control the resting membrane potential (Haimann et al., 1992; Koh et al., 1994; Bischoff et al., 1998). Recent evidence indicates that in adult medium-sized dorsal root ganglion (DRG) neurons, a single Na^+-dependent action potential can elicit a K_{Na} current, and K_{Na} channels were suggested to regulate the depolarizing after potential (DAP) (Gao et al., 2008). However, it has been difficult to reconcile these diverse physiological functions with one apparent property of K_{Na} channels: their requirement for high concentrations of $[Na^+]_i$ to activate. The normal resting level of $[Na^+]_i$ in neurons lies between 4 and 15 mM (Rose, 2002), and the effective concentrations required to activate 50% of channels (EC_{50}) have mostly been reported to range between 40 and 80 mM (Dryer, 1994), although some groups have reported much lower EC_{50}s (Haimann et al., 1990; Dale, 1993). The two genes that encode K_{Na} channels, *Slack* (*Slo 2.2, kcnt1*) and *Slick* (*Slo 2.1, kcnt2*) (Bhattacharjee and Kaczmarek, 2005; Salkoff et al., 2006), when expressed in CHO (Chinese hamster ovary) cells have EC_{50}s of ~40 and ~80 mM, respectively (Bhattacharjee et al., 2003). Although it has been suggested that transient elevations of Na^+ could reach in the tens of millimolars if a high density of Na^+ channels are present and the space is diffusionally restricted such as the node of Ranvier (Koh et al., 1994), quantitative models based on the diffusion equation suggest that the somatic concentration of Na^+ in the vicinity of the K_{Na} channels cannot reach this level, even if K_{Na} channels are assumed to be closely associated with Na^+ channels (Dryer, 1994). This raises the following question: are K_{Na} channels physiologically relevant, or are they only important during pathological states where $[Na^+]_i$ can accumulate rapidly such as hypoxia (Yuan et al., 2003)?

Na^+ dose–response relationships for K_{Na} channels have been established primarily through excised-patch recordings, because the presumed Na^+-binding site likely resides on the cytoplasmic face of the channel. By nature, the excised-patch configuration removes channels out from their native environment; in the case of K_{Na} channels, this experimental approach may not allow for an accurate assessment of what the normal Na^+ sensitivity of these channels might be. For example, when recording K_{Na} channels from intact cultured trigeminal neurons using the cell-attached configuration, K_{Na} channels exhibited a higher open probability compared with excised-patch recordings (Haimann et al., 1992). In addition, the high initial activity seen in cell-attached patches rapidly decreased after patch excision suggesting that a diffusible cytoplasmic factor likely regulates the activity of channels in intact neurons (Haimann et al., 1992). Similarly, in both rat and chick olfactory neurons, K_{Na} channels exhibited a rapid "rundown" after patch excision (Egan et al., 1992; Dryer, 1993), and

Received Feb. 19, 2009; revised March 19, 2009; accepted March 22, 2009.

This study was supported by a Junior Faculty Award from the American Diabetes Association to A.B. We thank Dr. Elsa Daurignac for critical reading of this manuscript.

Correspondence should be addressed to Dr. Arin Bhattacharjee, The State University of New York at Buffalo, 102 Farber Hall, 3435 Main Street, Buffalo, NY 14214. E-mail: ab68@buffalo.edu.

DOI:10.1523/JNEUROSCI.0859-09.2009

 0270-6474/09/295127-08$15.00/0

this rundown was also thought to occur as a result of the diffusion away of some unknown factor modulating K_{Na} channels (Egan et al., 1992). Thus, it is very plausible that K_{Na} channels in their native environment are activated by lower, physiological-relevant $[Na^+]_i$ compared with channels recorded in excised patches (Dryer, 2003).

Among DRG neurons, K_{Na} channels have only been studied in rat neonatal small DRG neurons (Bischoff et al., 1998) or in adult medium-sized DRG neurons (Gao et al., 2008). In this study, we show that Slack K_{Na} channels are ubiquitously expressed in adult rat DRG neurons. We also determine that the Na^+ dose–response relationship of K_{Na} channels in both small and large DRG neurons exhibited rundown during initial patch excision. Using sequence analysis, we discovered an NAD^+-binding site in the cytoplasmic terminal of the Slack channel and found that NAD^+ can activate both neuronal K_{Na} channels and Slack channels expressed in human embryonic kidney-293 cells. Modulation of K_{Na} channels by NAD^+ may now explain how these channels can participate in normal neuronal signaling.

Materials and Methods

Neuronal preparation. Adult rat DRG neurons were dissected and dissociated in 0.28 Wünsch units/ml Liberase Blendzyme (Roche Diagnostics Corporation) for 1 h at 37°C followed by washes in Hanks' buffered saline and trituration. Neurons were plated on poly-D-lysine and laminin (Sigma-Aldrich)-coated coverslips. Dissociated neurons were allowed to settle for 2 h before recording and were then used for up to 2 d. Neurons were cultured in Neurobasal-A medium (Invitrogen) supplemented with B-27 supplement (Invitrogen), L-glutamine (Invitrogen), and nerve growth factor (Harlan) and stored in a humidified incubator in 5% CO_2 at 37°C. Large neurons were classified with diameters >50 μm, and small neurons were classified with diameters <25 μm. Proprioceptive and nociceptive DRG neurons are usually designated as large and small, respectively. Overall assumptions in this classification are based on previous work examining conduction velocity versus the size of the neuron (Harper and Lawson, 1985). Neurons that fell outside this range were not recorded because of the possibility the neuron could be either proprioceptive or nociceptive.

DRG immunohistochemistry. Lumbar and thoracic DRGs were isolated from adult male (200 g) Sprague Dawley rats. Animals were anesthetized with sodium pentobarbital (60 mg/kg), perfused transcardially with 60 ml of PBS containing heparin (50 μg/ml) and sodium nitrite (5 mg/ml) followed by 60 ml of cold 4% paraformaldehyde. DRGs were removed, cleaned of surrounding tissue, postfixed in 4% paraformaldehyde, and transferred to 20% sucrose. After embedding in freezing media, frozen 20 μm sections of DRG were made. Slices were permeabilized with a PBS solution containing 0.4% Triton X-100. Sections were then blocked for 2 h at room temperature with PBS containing 5% BSA. Then sections were incubated with a mixture of primary antibodies in PBS containing 5% BSA overnight at 4°C. Primary antibodies included mouse anti-neurofilament antibody (1:400; Millipore Bioscience Research Reagents), calcitonin gene-related peptide (CGRP) antibody (1:2500; Sigma), and chicken anti-Slack antibody (1:1000) (Bhattacharjee et al., 2002). After several rinses, secondary antibodies Alexa Fluor 633 goat anti-mouse, Alexa Fluor 488 goat anti-rabbit, and Alexa Fluor 546 goat anti-chicken were added (1:1000) for 2 h. Coverslips were then mounted on slides using Prolong Gold antifade reagent with 4′,6′-diamidino-2-phenylindole dihydrochloride.

Cell culture. Human embryonic kidney (HEK-293) cells that stably express Slack channels (Yang et al., 2006) were a kind gift from Dr. Fred Sigworth (Yale University, New Haven, CT). Cells were cultured on 35 mm dishes in modified low Na^+ DMEM medium (Yang et al., 2006) containing 10% fetal bovine serum and penicillin-streptomycin (Invitrogen) and maintained in a 5% CO_2 incubator at 37°C.

Electrophysiology and analysis of data. All recordings were performed at room temperature. Electrodes resistances for excised-patch recordings ranged between 9 and 13 MΩ. Data was acquired using an Axopatch 200B (Molecular Devices), digitized, and filtered at 2 kHz and by using pCLAMP 9.2 (Molecular Devices) acquisition software. Data analysis was performed using Clampfit (Molecular Devices) and Origin 6.0 (OriginLab). Statistical analysis was performed using GraphPad Prism 4. Data are expressed as mean ± SE. Unpaired Student's *t* tests and one-way ANOVA analysis were used to determine statistical significance. For inside-out patch-clamp recordings, the pipette solution contained (in mM, unless specified otherwise) 10 NaCl, 130 KCl, 10 HEPES, 5 EGTA, 1 $MgCl_2$, and 1 tetraethylammonium chloride (TEA-Cl). The bath solution contained 130 KCl, 10 NaCl, 10 HEPES, and 5 EGTA. Solutions for patch-perfusion experiments to determine Na^+ dependency of channels were prepared as follows: equivalent solutions of 140 KCl, 140 NaCl, and 140 *N*-methyl glucamine (NMG)-Cl, and corresponding constituents (i.e., HEPES, EGTA) were made first. Starting solutions were then mixed to obtain the desired final ion concentration. The K^+ concentration was kept constant at 40 mM; NMG was used as cationic substitute to maintain osmolarity. Therefore, the highest Na^+ concentration we could use in our system was 100 mM. Cl^- concentrations were kept constant (140 mM) throughout the experiments. The pH of all solutions was adjusted to 7.3 with KOH. Inside-out patches were perfused with the SmartSquirt small volume delivery system (Automate Scientific) using a 100 μM perfusion tip with a flow rate of 0.01 ml/min, and varying concentrations of Na^+ were used in the perfusion. The free-acid form of β-nicotinamide adenine dinucleotide (β-NAD) was purchased from Fluka Biochemika and similarly β-NADP, β-NADH α-NAD, and oxidized glutathione (GSSG) from Sigma-Aldrich. Dose–response curves of Na^+, Na^+, and NAD^+ were fit to the equation $I = I_{min} + I_{max}/[1 + (C_{50}/C)^n]$, where I is the measured current density, I_{min} is the minimal current density, I_{max} is he peak current density, C is the concentration of agonist used, C_{50} is the concentration of agonist required to achieve half maximal activation (i.e., EC_{50}), and n is the degree of cooperativity. For tracking channel rundown time courses, the Savitzky–Golay smoothing algorithm was used to filter irregularities in data and perform a local polynomial regression for several data points. Relative maxima, minima, and width are preserved using this filtering algorithm.

For cell-attached recordings, the bath solution contained 140 NaCl, 3 KCl, 1 $CaCl_2$, 1 $MgCl_2$, and 25 HEPES. Pipette solution contained 10 NaCl, 140 KCl, 1 TEA-Cl, 1 μM tetrodotoxin (BIOMOL International), and 10 HEPES.

Site-directed mutagenesis. Mutation of the putative NAD^+ site was performed using sense and antisense primers designed against the putative NAD^+-binding region of the Slack channel cDNA in pTRACER. In the primer pair, one base mismatch was included to alter the final sequence that was obtained by PCR of a given cDNA by Pfu Turbo. PCR products were digested with *Dpn*I to eliminate nonamplified cDNA, and the remaining products were used to transform *Escherichia coli*. Miniprep DNA was then sequenced to verify that the designated changes had been made. Glycine 792 was mutated to alanine (G792A).

HEK-293 cells were cultured in DMEM containing 10% fetal bovine serum and penicillin-streptomycin. Cells were plated on plastic 35 mm dishes at a confluence of 20% and then transiently transfected with 0.9 μg of Slack G792A cDNA and 0.1 μg of CD8 a (lymphocyte cell-surface antigen) cDNA and 5 μl of Lipofectamine (Invitrogen). Recordings were performed 1–3 d after transfection. Transfected cells were identified by their binding to CD8-coated beads (Dyna-beads M-450 CD8).

Results

Ubiquitous Slack expression in adult DRG neurons

Using a previously characterized antibody against Slack channels (Bhattacharjee et al., 2002), we found Slack immunoreactivity in all types of rat DRG neurons (Fig. 1). Using confocal microscopy, we sampled an entire DRG and found Slack labeling in >90% of the neurons (Fig. 1*A*). Staining was positive for all neurons examined; for example, in small and medium CGRP-positive neurons, equally high levels of Slack immunoreactivity were found as in small CGRP-negative neurons. Slack labeling was also strong in large diameter neurons that were positive for neurofilamin (a marker of myelinated neurons), as demonstrated by the pinkish-

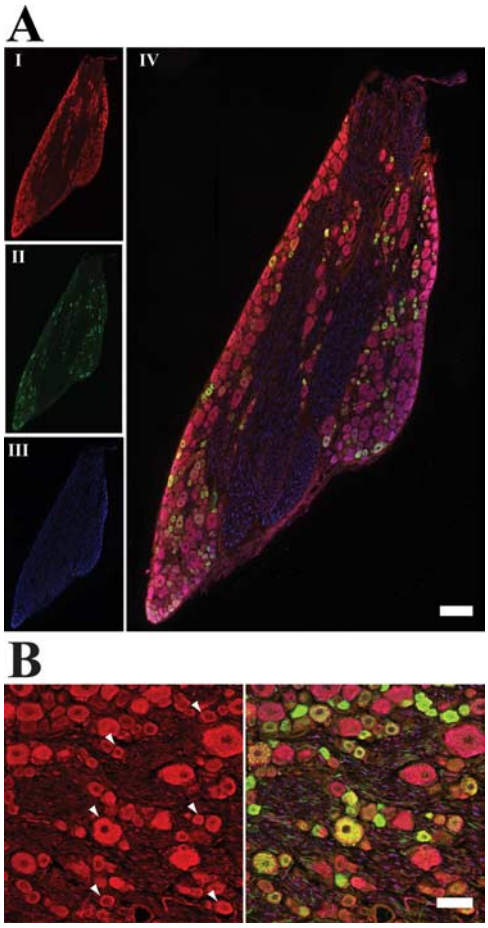

Figure 1. Slack is ubiquitously expressed in adult rat DRG. ***A***, Whole DRG staining. Multiple lower magnification single confocal images were compiled together into a single image representing an entire rat DRG. ***I***, Slack; ***II***, CGRP; ***III***, neurofilament; ***IV***, overlay of ***I–III***. More than 90% DRG neurons had Slack staining. ***B***, Higher magnification. Cell bodies and axons exhibited Slack labeling. Arrowheads indicate cell surface localization. Scale bars: ***A***, 200 μm; ***B***, 50 μm.

purple labeling in overlapping images (Fig. 1*A*,*B*). During examination at higher magnification, we found that Slack channels localized at the cell surface of DRG somata and within axonal tracts (Fig. 1*B*). Control experiments included incubating DRGs with the secondary antibody alone and with the antibody preabsorbed with blocking peptide (data not shown). Slack is widely distributed and not confined to one DRG neuronal subtype. We also found Slick channel immunoreactivity in adult DRG somata; however, there was differential labeling in small- and medium-sized DRG neurons versus large-sized DRG neurons (data not shown), suggesting that Slick channels may have a unique physiological role in nociception.

K_{Na} channels in DRG neurons

Adult DRG neurons were acutely dissociated and recorded within 2–24 h after plating. Neurons were categorized as either "large" or "small" based on diameter size (large >50 μm; small <25 μm). Using the cell-attached configuration, we recorded large conductance K_{Na}-like channel activity from acutely dissociated small (Fig. 2*A*) and large DRG neurons (data not shown) bathed in physiological saline ($n = 4$ for both). Channels were confirmed to be K_{Na} channels after excision and demonstration of Na^+ dependence (Fig. 2*A*). Channels typically had large unitary conductance (~200 pS) (Fig. 2*B*) and exhibited multiple subconductance states. Our data are very similar to that reported

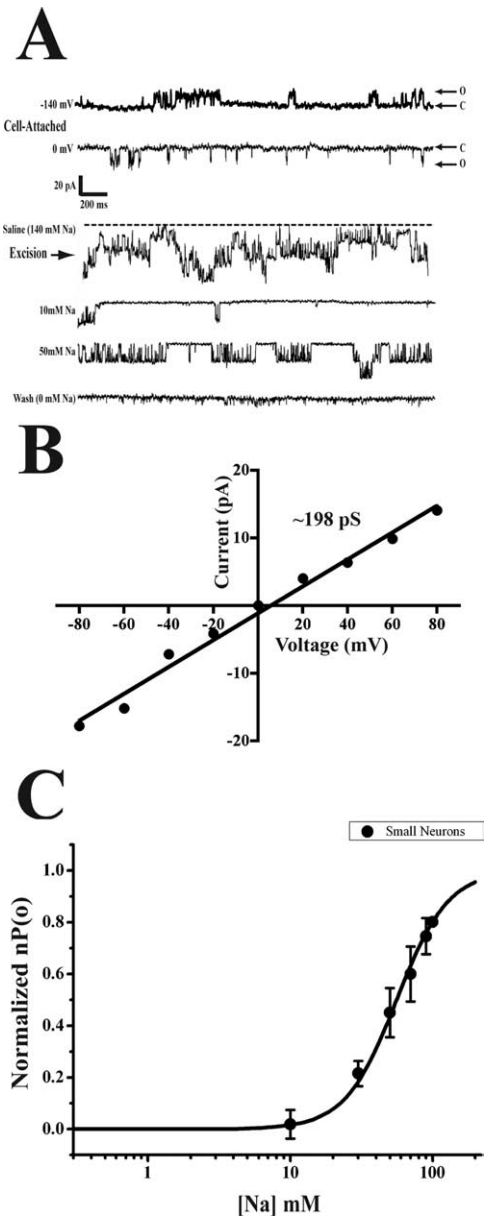

Figure 2. K_{Na} channels recorded from adult small DRG neurons. ***A***, Large conductance "K_{Na}-like" channels recorded in cell-attached patches on small DRG neurons bathed in physiological saline (140 mM Na^+ and 3 mM K^+). Pipette solution contained 130 mM K^+ and 1 mM TEA. Voltage indicated is the applied pipette potential. Excision into high external Na^+ confirmed K_{Na} channels. Patches were subsequently perfused with varying concentrations of Na^+ to confirm Na^+ dependence. Channels here were recorded at holding potential of −80 mV. ***B***, Current–voltage relationship in symmetrical K^+ revealed a large conductance channel. ***C***, Na^+ dose–response in small neurons ($n = 6$). EC_{50}, 53 mM; Hill coefficient, 2.4.

by Haimann et al. (1992) who recorded K_{Na} channels at rest in avian trigeminal neurons using cell-attached patches. These would suggest K_{Na} channels could contribute to physiological excitability.

To further characterize Na^+ dependence, inside-out patches were excised from neuronal somata and perfused with increasing concentrations of Na^+. Large conductance, Na^+-dependent K^+ channels were found in nearly three-quarters of patches excised from both small and large DRG neurons. Patches typically contained 3–5 channels. The pipette solution contained 1 mM TEA and was devoid of Ca^{2+} (contained 5 mM EGTA) as was the bath solution. This high expression correlates with our Slack immu-

nohistochemical data and is similar to what has been reported earlier (Bischoff et al., 1998; Gao et al., 2008). The K_{Na} channel EC_{50}s for Na^+ was determined to be 53 mM ($n = 6$) and 55 mM ($n = 6$) in small neurons (Fig. 2*C*) and large neurons (supplemental Fig. 1, available at www.jneurosci.org as supplemental material), respectively, and each with a Hill coefficients of 2.4.

K_{Na} channels exhibit rundown after patches are excised from somata

In some of the patches that were excised from small DRG neurons, we observed a high basal activity followed by a time-dependent decline in activity (Fig. 3*A*). Neurons were initially bathed in a 130 mM K^+, 10 mM Na^+-containing solution. We observed this rundown, which occurred within ~90 s after excision (Fig. 3*B*), in at least half of the patches recorded (3 of 6) from small neurons and in 1 of 6 large neurons. We retrospectively analyzed the data by averaging the three recordings taken from the small DRG neurons during initial excision and tracked the time course of rundown followed by the perfusion of patches with varying concentrations of Na^+. Because the initial activity was very different for each of the three patches, and had differing time course of rundown, to adjust for the scatter, the data was filtered using the Savitzky–Golay smoothing algorithm. Note that channel activity could be restored with increasing concentrations of Na^+, although very high concentrations of Na^+ were required to match the activity that was seen during the initial excision (Fig. 3*B*). This rundown phenomenon is similar to the rundown of K_{Na} channels recorded from olfactory neurons (Egan et al., 1992; Dryer, 1993) and trigeminal neurons (Haimann et al., 1992). In these previous reports, rundown was suggested to occur as the result of the diffusion away of some unknown factor modulating K_{Na} channels allowing the channels to exhibit activity at basal $[Na^+]_i$ conditions.

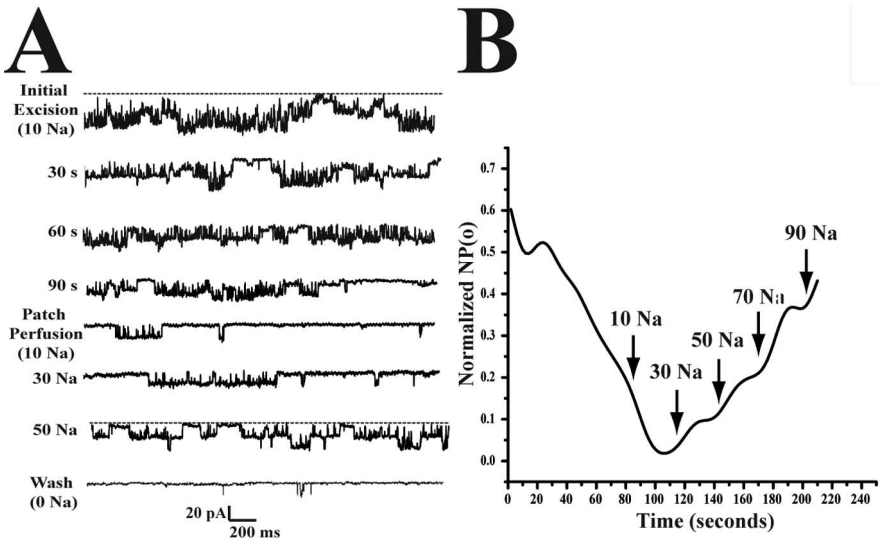

Figure 3. Rundown of K_{Na} channels after patch excision. ***A***, Representative traces of high basal K_{Na} channel activity. Rundown occurred in three of six patches from small DRG neurons. ***B***, NP(o) values were calculated for three patches every 2 s after patch excision in inside-out configuration. Channels were recorded at −80 mV. The nP(o)s were averaged after every 10 s, normalized to highest nP(o) in each neuron, and the averages for each time point were taken. Arrows indicate approximate commencement of perfusion of patches at each concentration of Na^+ (all values in millimolars). A Savitzky–Golay smoothing curve was used to filter data.

Slack and Slick channels contain a putative NAD^+-binding site

A modulating factor that increases the sensitivity of K_{Na} channels to Na^+ is an attractive idea, but a variety of cytoplasmic factors including cAMP, cGMP, ATP, cAMP-dependent protein kinase with ATP, protein kinase C, and pertussis toxin have been tested and none of these caused facilitory effects on native K_{Na} channels (Egan et al., 1992). We examined the secondary structure of the C terminal of both Slack and Slick using the secondary prediction program JPred3 from the University of Dundee (Dundee, UK; http://www.compbio.dundee.ac.uk/~www-jpred/) and the domain prediction software SBASE (Trieste, Italy; http://hydra.icgeb.trieste.it/~kristian/SBASE/). SBASE predicted that both Slack and Slick channels contain TrkA-N-like domains in their respective distil C termini. TrkA is a prokaryotic transporter that that binds NAD^+ at its N-terminal domain (TrkA N) (Schlösser et al., 1993). Canonical NAD^+-binding motifs have particular criteria for binding NAD^+. This binding motif includes a "fingerprint region" containing a $\beta\alpha\beta\alpha\beta$ motif of protein folding. In addition, the nucleotide-binding site must fit the following criteria: (1) A glycine-rich, phosphate-binding consensus sequence of GXGXXG which connects the β1 stand to the α1 helix; (2) six positions usually occupied by small hydrophobic amino acids; (3) a conserved, negatively charged residue at the end of the second β strand; and (4) a conserved positively charged residue at the beginning of the first β strand (Bellamacina, 1996). Using the predicted structural information from JPred3 and the hallmarks for nucleotide binding, we have compiled the structure of putative NAD^+-binding sites residing within the second RCK (regulate the conductance of K^+) domains of the Slack and Slick subunits, respectively, and compared them to known NAD^+-binding sites from prokaryotic K^+ transporters (Roosild et al., 2002) (Fig. 4). The third glycine of the GXGXXG phosphate consensus sequence is missing from Slack and Slick putative NAD^+-binding sites; however, this third glycine has been replaced by bulkier residues in other proteins that have the capability of binding the phosphorylated form of NAD^+, namely $NADP^+$. It is believed that a bulkier amino acid residue is required here to allow the phosphate group of $NADP^+$ to bind (Bellamacina, 1996).

NAD^+, but not NADH, modulates K_{Na} channels in DRG neurons

We subsequently tested if NAD^+ regulates native K_{Na} channels in DRG neurons. We assessed the K_{Na} channel Na^+ dose–response relationship in excised patches from small DRG neurons in the presence and absence of 1 mM NAD^+ in the perfusate (Fig. 5) ($n = 6$). Again, we identified K_{Na} channels using the criteria of conductance, subconductance states, and Na^+ dependence. Patches were first perfused with increasing concentrations of Na^+ and then the same patches were perfused with the same increasing Na^+ concentrations plus 1 mM NAD^+ (Fig. 5*A*). We consistently observed higher open probabilities in the presence of NAD^+ versus the absence of NAD^+. During these experiments, we did not obtain single channels; instead, patches contained multiple channels per

```
                    β1          α1          β2          α2          β3
Slack          -GFKNKLIIVSAETAGNGLYNFIVPLRAYYRSRRELNPIVLLLDNKPDHHFLEAICCFPMVYYME 839
Slick          -GFKNKLIIVAAETAGNGLYNFIVPLRAYYRPKKELNPIVLLLDNPPDMHFLDAICWFPMVYYMV 785
KtrAMja        ••••••MYIIIA----GIGRVGYTLAKSLSEKGHD-----IVLIDIDKDICKKASAEID-ALVING 50
KtrABsu        MGRIKNKQFAVI----GLGRFGGSIVKELHRMGHE-----VLAVDINEEKVNAYASYA--THAVIA 55
KtrAVal        •MKTGDKQFAVI----GLGRFGLAVCKELQDSGSQ-----VLAVDINEDRVKEAAGFV--SQAIVA 54
TrkABacF N-term     MKIIIA-----GAGAVGTHLAKLLSREKQD-----IILMDDDEEKLSTLSSNF-DLMTVTA 50

                    α3          β4          α4          β5
Slack          GSVDNLDSLLQCGIIYADNLVVVDKESTMSAEEDYMADAKTIVNVQTMFRLFPSLSITTELTHPSN 905
Slick          GSIDNLDDLLRCGVTFAANMVVVDKESTMSAEEDYMADAKTIVNVQTLFRLFSSLSIITELTHPAN 851
KtrAMja        DCTK-IKTLEDAGIEDADMYIAVTG---------KEEVNLMSSLLA--KSYGINKTIARISEIE-- 102
KtrABsu        NAT-EENELLSLGIRNFEYVIVAIG---------ANIQASTLTTLL--LKELDIPNIWVKAQNY-- 107
KtrAVal        NCT-HEETVAELKLDDYDMVMIAIG---------ADVNASILATLI--AKEAGVKSVWVKANDR-- 106
TrkABacF N-term SPSSI-SGLKEVGIKEADLFIAVTP--------DESRNMTACMLATNLGAEKTVARIDNYEYLLP- 106
```

Figure 4. Slack and Slick contain putative NAD^+-binding sites. NAD^+-binding sequence in Slack, Slick, and known NAD^+-dependent K^+ transporters from *Methanocaldococcus jannaschii* (Mja), *Bacillus subtilis* (Bsu), *Vibro alginolyticus* (Val), and *Bacteroides fragilis* (BacF). Yellow highlights indicate β sheets, whereas red highlights indicate α helices. The fingerprint region consists of a $\beta\alpha\beta\alpha\beta$ structure. The first green highlights indicated the conserved positive charge in beginning of the first β sheet in the fingerprint region. The second green highlights indicate the conserved negatively charged residue at the end of the second β sheet in the fingerprint region. The blue highlights are the phosphate-binding consensus sequence "GXGXXG" connecting the first β sheet to the first α helix. The purple highlights a consensus protein kinase C phosphorylation site present in Slack but not in Slick.

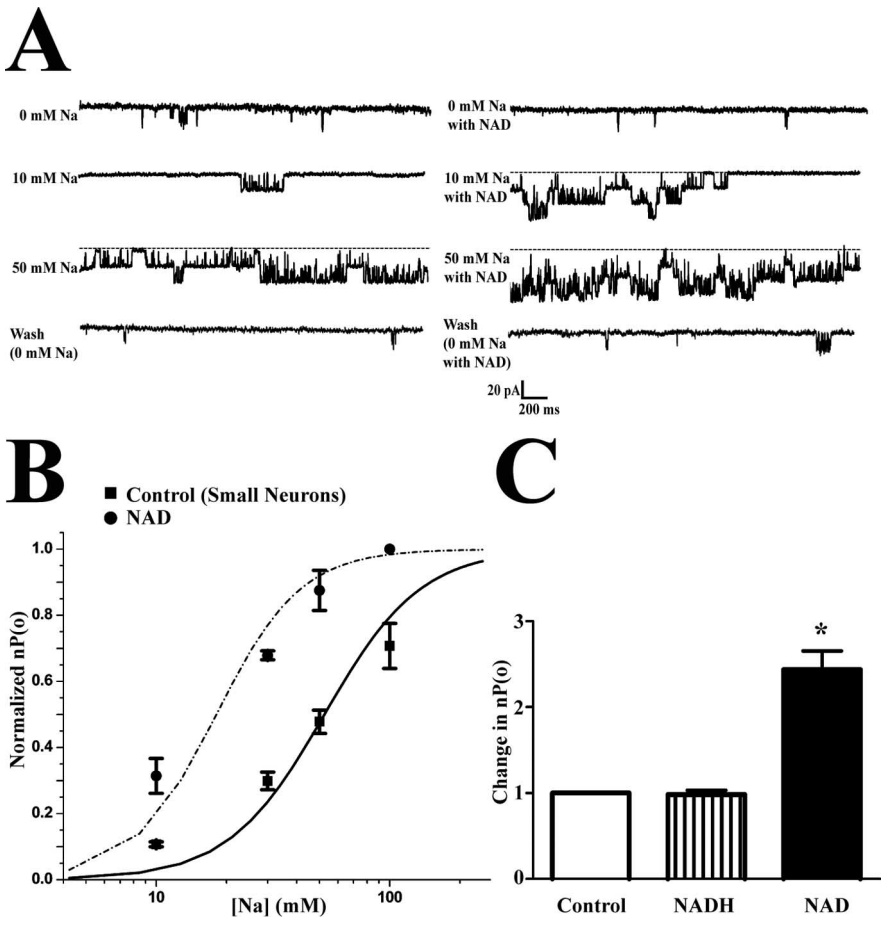

Figure 5. NAD^+ modulates K_{Na} channels in small DRG neurons. ***A***, Representative trace of channels recorded in an inside-out-excised patch from a small DRG neuron with X mM Na^+ (control) and with X mM Na^+ and 1 mM NAD^+. Voltage held at −80 mV. ***B***, Na^+ dose–response relationship of control and NAD^+ perfusions in small adult rat DRG neurons. NP(o) values were calculated from 30 sweeps of 2400 ms time samples at each dose of Na^+ and Na^+/NAD^+ solution. Each point represents an $n = 6$. Error bars represent SEM. EC_{50} was determined to be 50 mM for Na^+ and 17 mM for Na^+/NAD^+ solutions in small adult DRG neurons with a Hill coefficient of 2.4. ***C***, NADH does not modulate K_{Na} channel activity in DRG neurons. Na^+ (30 mM; control) was perfused onto inside-out-excised patches and compared with 30 mM Na^+ + 1 mM NADH and 30 mM + 1 mM NAD^+. Voltage was held at −80 mV. NP(o) values were calculated from 30 sweeps of 2400 ms time samples ($n = 5$; *$p < 0.01$). Error bars represent SEM.

patch; however, we did not observe any changes in unitary conductance nor did we see changes in open times (210 ± 40 ms in 10 mM Na; 192 ± 37 ms in 10 mM Na^+ + 1 mM NAD^+). The Na^+ dose-dependent relationship and Na^+/NAD^+ dose-dependent relationship was established in small DRG neurons, and we observed a leftward shift in the presence of NAD^+ (Fig. 5*B*). In these experiments, EC_{50} was estimated to be ~52 mM, whereas in the presence of NAD^+, the EC_{50} was calculated to be ~20 mM. We similarly observe NAD^+ facilitation of K_{Na} channels recorded from large DRG neurons (supplemental Fig. 2, available at www.jneurosci.org as supplemental material). Note that NAD^+ in the absence of Na^+ did not affect channel activity.

We next determined if the reduced form of NAD^+, namely NADH, could also modulate the open probability of the channel. Although NAD^+ and NADH are structurally very similar, the NADH consensus-binding site is considered to be GXGXXGXXXGXXXXG (Scrutton et al., 1990). We perfused several inside-out-excised patches from small neurons ($n = 5$) with solutions containing 30 mM Na^+ with and without NADH. We found no significant change in open probability versus the control, whereas native channels perfused with NAD^+ exhibited a significant 2–2.5-fold increase in open probability (Fig. 5*C*) ($p < 0.01$).

NAD^+ and $NADP^+$, but not NADH nor αNAD, modulate Slack channels

Since at present the precise molecular composition of native K_{Na} channels in DRG neurons is unknown, we tested if NAD^+ also modulated recombinant Slack channels. We performed similar inside-out-excised patch-perfusion experiments on Slack channels recorded from a Slack-stable HEK-293 cell line. Inside-out-excised patches were perfused with 10 mM Na^+, followed by 10 mM Na^+ and 1 mM NAD^+, or 1 mM $NADP^+$ (Fig. 6*A*,*B*). Because of the high expression of Slack channels in this cell line, we used a lower concentration of Na^+ (10 mM) to study Slack channel open probability. We also did not observe Slack channel run down after patch excision. Similar to the neurons, however, we did see a statistically significant twofold increase in Slack channel open probability in the presence of NAD^+ and a statistically significant 1.5-fold increase in the presence of $NADP^+$. We did not observe a change in open probability when NADH was included in the perfusate (Fig. 6*A*,*B*,*E*) ($n = 6$ for NAD^+, $n = 5$ for $NADP^+$, and $n = 5$ for NADH), nor was their an effect using the αNAD^+ stereo iso-

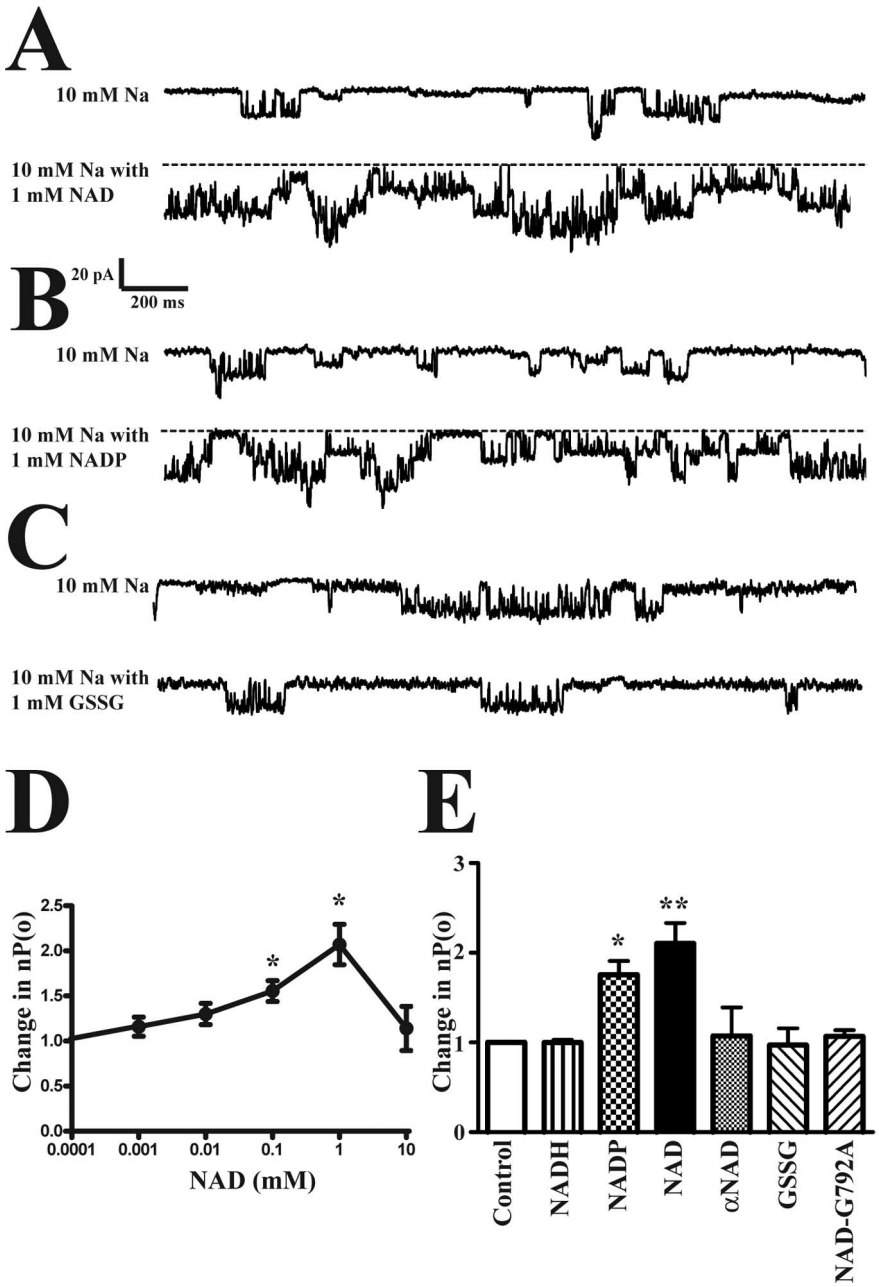

Figure 6. NAD^+ and $NADP^+$ modulate Slack channels stably expressed in HEK-293T. ***A***, Representative traces of NAD^+-activating recombinant Slack channels. ***B***, Representative traces of $NADP^+$-activating recombinant Slack channels. ***C***, Representative traces of GSSG failing to activate recombinant Slack channels. All voltages held at −80 mV. Excised patch recordings were performed from a Slack-stable-transfected HEK-293 cell line. ***D***, NAD^+ dose–response relationship on Slack channels. Each perfusion contained X mM NAD^+, 10 mM Na^+, 40 mM K^+, 90 mM NMG. *$p < 0.01$, statistical significance compared with control. ***E***, Summary of the effects of NADH, $NADP^+$, NAD^+, αNAD^+, the oxidizing agent, GSSG, on Slack channels and NAD^+ on a Slack G792A mutant channel versus the control. The Slack mutant was generated through by site-directed mutagenesis of second glycine in NAD^+ fingerprint region. All solutions contained 1 mM of either NAD^+, NADH or $NADP^+$, αNAD^+, GSSG, and 10 mM Na^+, 40 mM K^+, 90 mM NMG. *$p < 0.005$ and **$p < 0.001$, significant difference versus control. Error bars represent SEM.

mer of NAD^+ (Fig. 6*E*) ($n = 3$). These data confirm that NAD^+ and $NADP^+$ act on Slack channels as well.

NAD^+ effects on Slack channels are likely not attributable to oxidation

Although our evidence to this point strongly suggested that NAD^+ was acting by allosterically modulating Slack channels, we could not be sure that NAD^+ was acting by oxidizing Slack channels. To confirm that the NAD^+ effects are direct and not attributable to oxidation, we applied 1 mM of the oxidized form of GSSG to patches. At this concentration, GSSG is a strong oxidizing agent (Ruddock et al., 1996). We found that 1 mM GSSG did not alter Slack channel open probability (Fig. 6*C*,*E*) ($n = 5$), suggesting that NAD^+ is probably allosterically affecting channels.

In general, NAD^+ concentrations within cells are much higher than NADH and $NADP^+$. The cellular concentration of NAD^+ has been estimated to be between 0.3 to 0.4 mM (Yamada et al., 2006; Yang et al., 2007), although the concentrations within neurons are not well established. We tested various concentrations of NAD^+ to evaluate the minimal concentrations of NAD^+ needed to cause a significant facilitation in open probability. We performed experiments on inside-out-excised patches of Slack channels from the same Slack-stable cell line using a fixed 10 mM Na^+ concentration and applying varying concentrations of NAD (0.001, 0.01, 0.01, 1, and 10 mM) (Fig. 6*D*) ($n = 5$). We observed a significant change in open probability at 0.1 mM NAD and 1 mM NAD ($n = 5$, $p < 0.005$ for each). Note, at 10 mM NAD, there was a significant and reversible decrease in channel activity ($n = 5$, $p < 0.001$). It seemed that the higher NAD^+ concentration might have been interfering with Na^+ binding and not blocking the channel because open probability was diminished and unitary conductance was not lowered (data not shown).

Finally, to confirm that NAD^+ was modulating the channel directly, we used site-directed mutagenesis to mutate the second glycine in the phosphate-binding region "GXGXXG" to an alanine, "GXAXXG." The second glycine, because of its missing side chain, allows for close contact of the main chain to the diphosphate of $NAD(P)^+$. It is thought that any side chain in this position would protrude into the binding site of $NAD(P)^+$ and disrupt cofactor binding (Bellamacina, 1996). We chose alanine accordingly to disrupt the binding site and not a bulky amino acid or charged amino acid that could have distorted overall protein conformation affecting channel functioning.

We transfected HEK-293 cells with the Slack G792A and conducted Na^+ and Na^+/NAD^+ perfusion experiments using inside-out-excised patches from transfected cells. We found no significant change in channel activity between the Na^+ perfusion

and the Na^+/NAD^+ perfusion on channels with the mutated NAD^+-binding site (Fig. 6*E*) ($n = 5$).

Discussion

In this study, using immunolabeling and electrophysiological analyses, we demonstrated that K_{Na} channels are abundantly expressed in adult rat DRG neurons. Previous work has documented that K_{Na} channels can be recorded in small- and medium-sized DRG neurons (Bischoff et al., 1998; Gao et al., 2008), and we have now demonstrated that K_{Na} channels are also present in large, proprioceptive DRG neurons. The Na^+-dose–response relationship for K_{Na} channels for both small and large DRG neurons was determined to be similar. We also showed that K_{Na} channels are active at rest and are modulated by the metabolic coenzyme NAD^+. The modulation by NAD^+ resulted in a K_{Na} channel Na^+ dependence that falls in the physiological $[Na^+]_i$ range for neurons. Because DRG neurons fire at modest frequencies (0.5–10 Hz), this modulation is highly pertinent; it will allow channels to operate under conditions where appreciable $[Na^+]_i$ accumulation is not expected to normally occur. NAD^+ did not modulate channels in the absence of Na^+. In the presence of Na^+, NAD^+ did not increase K_{Na} channel unitary conductance. It seemed that NAD^+ acted at the level of Na^+ binding; however, extensive single-channel analysis will be required to determine how NAD^+ modulates K_{Na} channels.

The results of our findings and those by Haimann et al. (1992) and Egan et al. (1992) underscore the idea that Na^+ sensitivity as measured by excised-patch recordings of K_{Na} channels likely does not reflect what the real Na^+ sensitivity might be when channels are situated in their native environment. We presume that channel rundown is the result of NAD^+ diffusing away from the patch. However, K_{Na} channel rundown has not been observed in all neurons (Dryer, 1993), and we certainly did not see rundown in all DRG neurons. There may be other factors influencing NAD^+ modulation such as the molecular composition of native K_{Na} channels and/or channel phosphorylation status. Indeed, there is a consensus protein kinase C (PKC) phosphorylation site in the heart of the NAD^+-binding site of Slack (Fig. 4), and whole-cell perforated-patch-recorded Slack currents are facilitated after PKC activation (Santi et al., 2006). It is not well established how PKC potentiates Slack channels. It could be that phosphorylation of the NAD^+-binding site enhances NAD^+ binding. This remains to be explored.

Beyond its role in metabolism, an integrative protective role for NAD^+ in neurons is starting to emerge. Numerous investigations have shown that when neurons are injured, they respond by upregulating NAD^+ biosynthetic enzymes, and NAD^+ protects neurons from subsequent neurodegeneration (Wang et al., 2005; Sasaki et al., 2006; Ying, 2007). Similarly, DRG neuronal dysfunction during nerve injury and/or diabetes has been attributed to decreases in NAD^+ levels (Ido, 2007; Sharma et al., 2008), which can result in neuropathic pain. Neuropathic pain is pain that arises from abnormal nervous system physiology, at times completely removed from ongoing tissue damage or inflammation (Stacey, 2005). In many instances, neuropathic pain occurs as a direct result of hyperexcitable DRG neurons. Indeed, streptozotocin, an NAD^+-depleting agent and pancreatic β-cell toxin, used to induce experimental diabetes in animal models, is directly toxic to sensory neurons resulting in measurable thermal hyperalgesia before hyperglycemia ensues (Pabbidi et al., 2008). These would suggest that a direct coupling might exist between resting NAD^+ levels and the intrinsic firing properties of DRG neurons.

Our data suggests that a decrease in DRG neuronal NAD^+ should result in an impaired modulation of K_{Na} channels and concomitant decreased Na^+ sensitivity of K_{Na} channels. K_{Na} channels, however, are not the only K^+ channels modulated by metabolic coenzymes. Precedence for modulation by NAD^+, $NADP^+$, or NADH has been set with a variety of K^+ channels, including the K^+ transport-nucleotide-binding channel, the ATP-sensitive K^+ channel, and the Ca^{2+}-activated K^+ channel (Lee et al., 1994; Roosild et al., 2002; Dabrowski et al., 2003; Tipparaju et al., 2005). If K_{Na} channels control DRG neuronal resting membrane potential (Bischoff et al., 1998) and/or limit the DAP (Gao et al., 2008), then reduced K_{Na} activity as a result of decreased NAD^+ modulation will lead to DRG neuronal hyperexcitability and spontaneous firing. As we have now shown, K_{Na} channels are abundantly and ubiquitously expressed in DRG neurons. Since both propioceptors and nociceptors are believed to contribute to painful neuropathy (Amir et al., 1999; Ma and LaMotte, 2007), K_{Na} channel dysfunctioning may be a likely culprit in the pathology of neuropathic pain. Alternatively, increasing K_{Na} channel activity may also represent a therapeutic strategy for the treatment of neuropathic pain.

References

Amir R, Michaelis M, Devor M (1999) Membrane potential oscillations in dorsal root ganglion neurons: role in normal electrogenesis and neuropathic pain. J Neurosci 19:8589–8596.

Bellamacina CR (1996) The nicotinamide dinucleotide binding motif: a comparison of nucleotide binding proteins. FASEB J 10:1257–1269.

Bhattacharjee A, Kaczmarek LK (2005) For K+ channels, Na+ is the new Ca2+. Trends Neurosci 28:422–428.

Bhattacharjee A, Gan L, Kaczmarek LK (2002) Localization of the Slack potassium channel in the rat central nervous system. J Comp Neurol 454:241–254.

Bhattacharjee A, Joiner WJ, Wu M, Yang Y, Sigworth FJ, Kaczmarek LK (2003) Slick (Slo2.1), a rapidly-gating sodium-activated potassium channel inhibited by ATP. J Neurosci 23:11681–11691.

Bischoff U, Vogel W, Safronov BV (1998) Na+-activated K+ channels in small dorsal root ganglion neurones of rat. J Physiol 510:743–754.

Dabrowski M, Trapp S, Ashcroft FM (2003) Pyridine nucleotide regulation of the KATP channel Kir6.2/SUR1 expressed in *Xenopus* oocytes. J Physiol 550:357–363.

Dale N (1993) A large, sustained Na(+)- and voltage-dependent K+ current in spinal neurons of the frog embryo. J Physiol 462:349–372.

Dryer SE (1993) Properties of single Na(+)-activated K+ channels in cultured central neurons of the chick embryo. Neurosci Lett 149:133–136.

Dryer SE (1994) Na(+)-activated K+ channels: a new family of large-conductance ion channels. Trends Neurosci 17:155–160.

Dryer SE (2003) Molecular identification of the Na+-activated K+ channel. Neuron 37:727–728.

Egan TM, Dagan D, Kupper J, Levitan IB (1992) Properties and rundown of sodium-activated potassium channels in rat olfactory bulb neurons. J Neurosci 12:1964–1976.

Gao SB, Wu Y, Lü CX, Guo ZH, Li CH, Ding JP (2008) Slack and Slick K_{Na} channels are required for the depolarizing afterpotential of acutely isolated, medium diameter rat dorsal root ganglion neurons. Acta Pharmacol Sin 29:899–905.

Haimann C, Bernheim L, Bertrand D, Bader CR (1990) Potassium current activated by intracellular sodium in quail trigeminal ganglion neurons. J Gen Physiol 95:961–979.

Haimann C, Magistretti J, Pozzi B (1992) Sodium-activated potassium current in sensory neurons: a comparison of cell-attached and cell-free single-channel activities. Pflugers Arch 422:287–294.

Harper AA, Lawson SN (1985) Electrical properties of rat dorsal root ganglion neurones with different peripheral nerve conduction velocities. J Physiol 359:47–63.

Ido Y (2007) Pyridine nucleotide redox abnormalities in diabetes. Antioxid Redox Signal 9:931–942.

Koh DS, Jonas P, Vogel W (1994) Na(+)-activated K+ channels localized

in the nodal region of myelinated axons of *Xenopus*. J Physiol 479:183–197.

Lee S, Park M, So I, Earm YE (1994) NADH and NAD modulates Ca(2+)-activated K+ channels in small pulmonary arterial smooth muscle cells of the rabbit. Pflugers Arch 427:378–380.

Ma C, LaMotte RH (2007) Multiple sites for generation of ectopic spontaneous activity in neurons of the chronically compressed dorsal root ganglion. J Neurosci 27:14059–14068.

Pabbidi RM, Cao DS, Parihar A, Pauza ME, Premkumar LS (2008) Direct role of streptozotocin in inducing thermal hyperalgesia by enhanced expression of transient receptor potential vanilloid 1 in sensory neurons. Mol Pharmacol 73:995–1004.

Roosild TP, Miller S, Booth IR, Choe S (2002) A mechanism of regulating transmembrane potassium flux through a ligand-mediated conformational switch. Cell 109:781–791.

Rose CR (2002) Na^+ signals at central synapses. Neuroscientist 8:532–539.

Ruddock LW, Hirst TR, Freedman RB (1996) pH dependence of the dithiol-oxidizing activity of DsbA (a periplasmic protein thiol:disulphide oxidoreductase) and protein disulphide-isomerase: studies with a novel simple peptide substrate. Biochem J 315:1001–1005.

Salkoff L, Butler A, Ferreira G, Santi C, Wei A (2006) High-conductance potassium channels of the SLO family. Nat Rev Neurosci 7:921–931.

Santi CM, Ferreira G, Yang B, Gazula VR, Butler A, Wei A, Kaczmarek LK, Salkoff L (2006) Opposite regulation of Slick and Slack K^+ channels by neuromodulators. J Neurosci 26:5059–5068.

Sasaki Y, Araki T, Milbrandt J (2006) Stimulation of nicotinamide adenine dinucleotide biosynthetic pathways delays axonal degeneration after axotomy. J Neurosci 26:8484–8491.

Schlösser A, Hamann A, Bossemeyer D, Schneider E, Bakker EP (1993) NAD+ binding to the *Escherichia coli* K+-uptake protein TrkA and sequence similarity between TrkA and domains of a family of dehydrogenases suggest a role for NAD+ in bacterial transport. Mol Microbiol 9:533–543.

Scrutton NS, Berry A, Perham RN (1990) Redesign of the coenzyme specificity of a dehydrogenase by protein engineering. Nature 343:38–43.

Sharma SS, Kumar A, Kaundal RK (2008) Protective effects of 4-amino1,8-napthalimide, a poly (ADP-ribose) polymerase inhibitor in experimental diabetic neuropathy. Life Sci 82:570–576.

Stacey BR (2005) Management of peripheral neuropathic pain. Am J Phys Med Rehabil 84:S4–S16.

Tipparaju SM, Saxena N, Liu SQ, Kumar R, Bhatnagar A (2005) Differential regulation of voltage-gated K+ channels by oxidized and reduced pyridine nucleotide coenzymes. Am J Physiol Cell Physiol 288:C366–C376.

Wang J, Zhai Q, Chen Y, Lin E, Gu W, McBurney MW, He Z (2005) A local mechanism mediates NAD-dependent protection of axon degeneration. J Cell Biol 170:349–355.

Yamada K, Hara N, Shibata T, Osago H, Tsuchiya M (2006) The simultaneous measurement of nicotinamide adenine dinucleotide and related compounds by liquid chromatography/electrospray ionization tandem mass spectrometry. Anal Biochem 352:282–285.

Yang B, Gribkoff VK, Pan J, Damagnez V, Dworetzky SI, Boissard CG, Bhattacharjee A, Yan Y, Sigworth FJ, Kaczmarek LK (2006) Pharmacological activation and inhibition of Slack (Slo2.2) channels. Neuropharmacology 51:896–906.

Yang H, Yang T, Baur JA, Perez E, Matsui T, Carmona JJ, Lamming DW, Souza-Pinto NC, Bohr VA, Rosenzweig A, de Cabo R, Sauve AA, Sinclair DA (2007) Nutrient-sensitive mitochondrial NAD+ levels dictate cell survival. Cell 130:1095–1107.

Ying W (2007) NAD+ and NADH in neuronal death. J Neuroimmune Pharmacol 2:270–275.

Yuan A, Santi CM, Wei A, Wang ZW, Pollak K, Nonet M, Kaczmarek L, Crowder CM, Salkoff L (2003) The sodium-activated potassium channel is encoded by a member of the Slo gene family. Neuron 37:765–773.